

Fig. 3.6 The evolution of an initial symmetric wave, which is imagined to be composed of three rectangular blocks with shorter blocks on top of longer blocks. The wave speeds of these fluid blocks are approximately equal to  $c_n = \sqrt{g(H + nh)}$ , based on shallow-water theory, where  $n = 1, 2,$  and  $3$ ,  $H$  is the shallow-water layer depth, and  $h$  is the height of an individual fluid block. The wave steepening in (b) and wave overturning in (c) are interpreted by the different wave speeds of different fluid blocks because  $c_3 > c_2 > c_1$ .

by imagining an elevated wave that is composed of several rectangular blocks with shorter blocks of fluid on top of longer blocks (Fig. 3.6a). Since the shallow water wave speed is proportional to the mean layer depth  $H$ , the speed of fluid particles in the upper layer will be greater than that in the lower layer. Thus, the wave front will have a tendency to steepen (Fig. 3.6b) and possibly overturn (Fig. 3.6c). Once overturning occurs, the fluid becomes statically unstable and turbulence will be induced.

In a rotating shallow water system, the Coriolis force becomes more and more important when the Rossby number decreases. In this situation, the fluid may undergo geostrophic adjustment to an initial disturbance, as briefly discussed in Chapter 1, to a scale determined by the Rossby radius of deformation,  $\lambda_R = c/f = \sqrt{gH}/f$ .

### 3.5 Pure gravity waves

Consider small-amplitude (linear) perturbations in a two-dimensional ( $\partial/\partial y = 0$ ), inviscid, nonrotating, adiabatic, Boussinesq, uniform basic state flow with uniform stratification, (2.2.14)–(2.2.18) reduce to

$$\frac{\partial u'}{\partial t} + U \frac{\partial u'}{\partial x} + \frac{1}{\rho_0} \frac{\partial p'}{\partial x} = 0, \quad (3.5.1)$$

$$\frac{\partial w'}{\partial t} + U \frac{\partial w'}{\partial x} - g \frac{\theta'}{\theta_0} + \frac{1}{\rho_0} \frac{\partial p'}{\partial z} = 0, \quad (3.5.2)$$

$$\frac{\partial u'}{\partial x} + \frac{\partial w'}{\partial z} = 0, \quad (3.5.3)$$

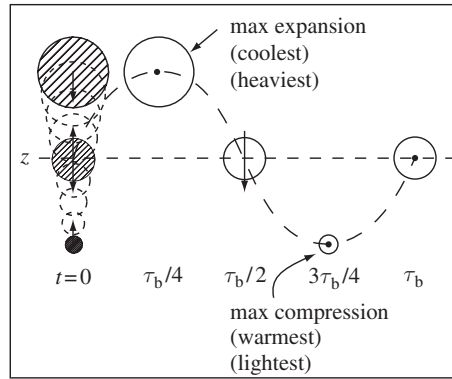


Fig. 3.7 Vertical oscillation of an air parcel in a stably stratified atmosphere when the Brunt–Vaisala frequency is  $N$ . The oscillation period of the air parcel is  $\tau_b = 2\pi/N$  and the volume of the air parcel is proportional to the area of the circle. (Adapted after Hooke 1986.)

$$\frac{\partial \theta'}{\partial t} + U \frac{\partial \theta'}{\partial x} + \frac{N^2 \theta_0}{g} w' = 0, \quad (3.5.4)$$

where  $\theta_0$  is a constant reference potential temperature, and  $N^2 (\equiv (g/\theta_0) \partial \bar{\theta} / \partial z)$  is the square of the Boussinesq Brunt–Vaisala (buoyancy) frequency. Figure 3.7 illustrates the vertical oscillation of an air parcel in a stratified atmosphere with a Brunt–Vaisala frequency  $N$ . The total oscillation period is  $2\pi/N$  ( $\tau_b$  in the figure). The air parcel expands and cools while it ascends, and reaches its maximum expansion and coolest state at  $t = \tau_b/4$ . At this level, the air parcel density perturbation is the largest. It then descends due to negative buoyancy and overshoots passing its original level at  $t = \tau_b/2$ . The air parcel compresses and warms adiabatically while it descends, and reaches its maximum compression and warmest state at  $t = 3\tau_b/4$ . At this level, the air parcel density perturbation is the lowest. It then ascends due to positive buoyancy, and returns to its original level at  $t = \tau_b$ . For a two-dimensional, nonrotating fluid flow, there is no need to retain the meridional ( $y$ -) momentum equation in our system of equations, because  $v'$  will keep its initial value for all time, as required by the reduced form of the  $y$ -momentum equation, namely,  $\partial v' / \partial t + U \partial v' / \partial x = 0$ . Note that the  $y$ -momentum equation needs to be kept if the fluid is two-dimensional and rotating since the initial  $v'$  will vary with time, although independent of  $y$ , due to the presence of the Coriolis force.

Equations (3.5.1)–(3.5.4) may be combined into a single equation for the vertical velocity  $w'$ , which is a simplified form of the Taylor–Goldstein equation [(3.7.19)] in the absence of vertical wind shear,

$$\left( \frac{\partial}{\partial t} + U \frac{\partial}{\partial x} \right)^2 \left( \frac{\partial^2 w'}{\partial x^2} + \frac{\partial^2 w'}{\partial z^2} \right) + N^2 \frac{\partial^2 w'}{\partial x^2} = 0. \quad (3.5.5)$$

Assuming a traveling sinusoidal plane wave solution of the form,

$$w' = \hat{w}(z) e^{i(kx - \omega t)}, \quad (3.5.6)$$

and substituting it into (3.5.5) yields the following linear partial differential equation with constant coefficients, which governs the vertical structure of  $w'$ ,

$$\frac{\partial^2 \hat{w}}{\partial z^2} + \left( \frac{N^2}{\Omega^2} - 1 \right) k^2 \hat{w} = 0. \quad (3.5.7)$$

In the above equation,  $\Omega \equiv \omega - kU$  is the *intrinsic (Doppler-shifted) frequency* of the wave relative to the uniform basic state flow. Equation (3.5.7) has the following two solutions:

$$\hat{w} = A e^{ik\sqrt{N^2/\Omega^2 - 1}z} + B e^{-ik\sqrt{N^2/\Omega^2 - 1}z}, \quad \text{for } N^2/\Omega^2 > 1, \quad (3.5.8)$$

and

$$\hat{w} = C e^{k\sqrt{1 - N^2/\Omega^2}z} + D e^{-k\sqrt{1 - N^2/\Omega^2}z}, \quad \text{for } N^2/\Omega^2 < 1. \quad (3.5.9)$$

Equation (3.5.8) represents a vertically propagating wave because it is sinusoidal with height. As will be discussed in Section 4.4, term  $A$  represents a wave with upward energy propagation, while term  $B$  represents a wave with downward energy propagation. Thus, for waves generated by orography, term  $B$  is unphysical and has to be removed because the wave energy source is located at the surface, as required by the *radiation boundary condition*. On the other hand, term  $C$  of (3.5.9) represents wave amplitude increasing exponentially with height, while term  $D$  represents a wave whose amplitude decreases exponentially from the level of wave generation. Thus, for waves or disturbances generated by orography, term  $C$  is unphysical. This is also called the *boundedness condition*. Under this situation, term  $D$  represents an evanescent wave or disturbance, whose wave amplitude decreases exponentially with height. In other words, there exist two distinct flow regimes for pure gravity waves (i.e. *vertically propagating waves* and *evanescent waves*) in the atmosphere, which are determined respectively by the following criteria:

$$N^2/\Omega^2 > 1 \quad \text{and} \quad N^2/\Omega^2 < 1. \quad (3.5.10)$$

The above two pure gravity wave flow regimes can be understood by considering steady-state responses of stably stratified airflow over a sinusoidal topography. In this particular case,  $\Omega^2 = k^2 U^2$ . When  $N^2/\Omega^2 > 1$ , we have  $2\pi/N < L/U$ , where  $L = 2\pi/k$  is the dominant horizontal wavelength of the sinusoidal topography. Note that  $2\pi/N$  is the buoyancy oscillation period and that  $L/U$  is the advection time an air parcel takes to cross over one wavelength of the mountain. Thus, fluid particles take less time to oscillate in the vertical, compared to the horizontal advection time required to pass over the mountain. This allows the wave energy to propagate vertically (Fig. 3.8a). On the other hand, when  $N^2/\Omega^2 < 1$  or  $2\pi/N > L/U$ , fluid particles do not have enough time to

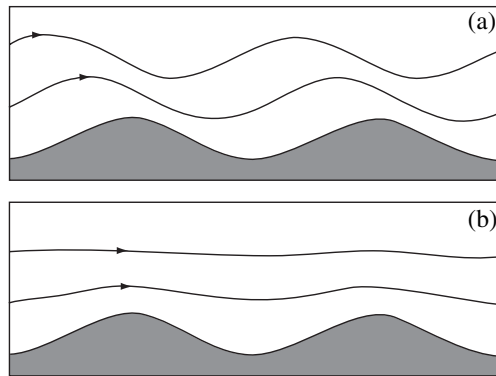


Fig. 3.8 (a) Vertically propagating waves and (b) evanescent waves for a linear, two-dimensional, inviscid flow over sinusoidal topography.

oscillate vertically because the time required for the particles to be advected over the mountain is shorter. Therefore, the wave energy cannot freely propagate vertically, and it is preferentially advected downstream, remaining near the Earth's surface (Fig. 3.8b). This type of wave or disturbance is also referred to as an evanescent wave or a *surface trapped wave*.

If the stratification of the fluid is uniform and the disturbance is sinusoidal in the vertical, then  $\hat{w}$  may be written as  $\hat{w} = w_0 e^{imz}$ , where  $w_0$  and  $m$  are the wave amplitude and vertical wave number, respectively. Substituting  $\hat{w}$  into (3.5.7) yields the dispersion relation for pure gravity waves,

$$\Omega = \frac{\pm Nk}{\sqrt{k^2 + m^2}}. \quad (3.5.11)$$

For a quiescent fluid ( $U=0$ ), the above equation reduces to

$$\omega = \frac{\pm Nk}{\sqrt{k^2 + m^2}}, \quad (3.5.12)$$

or

$$\frac{\omega}{N} = \frac{\pm k}{\sqrt{k^2 + m^2}} = \pm \cos \alpha, \quad (3.5.13)$$

where  $\alpha$  is the angle ( $|\alpha| \leq \pi/2$ ) between the wave number vector  $\mathbf{k} = (k, m)$  and the  $x$ -axis. While the wave number vector is oriented in the same direction as the phase speed vector ( $c_p$  in Fig. 3.9), the wave front is oriented perpendicular. Fluid parcels oscillate in a direction perpendicular to the total wave number vector, as indicated by the incompressible continuity equation,  $\mathbf{k} \cdot \mathbf{V}' = 0$ . Therefore, the wave fronts or rays associated with particle oscillations tilt at an angle  $\alpha$  with respect to the vertical. This characteristic behavior of nonrotating internal gravity waves has been verified in water tank experiments (Mowbray and Rarity 1967). For a given stratification,

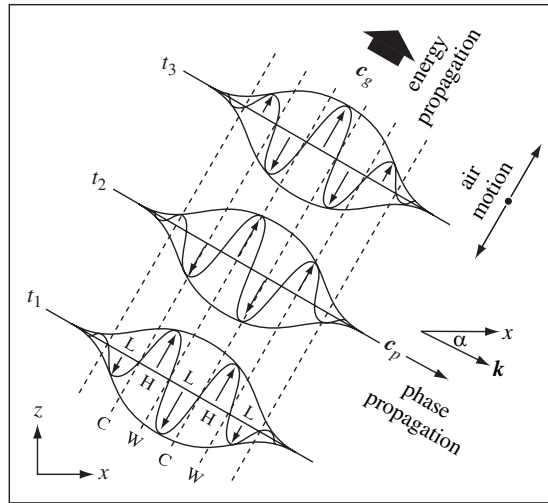


Fig. 3.9 Basic properties of a vertically propagating gravity wave with  $k > 0$ ,  $m < 0$ , and  $\omega > 0$ . The energy of the wave group propagates with the group velocity ( $c_g$ ; thick blunt arrow), while the phase of the wave propagates with the phase speed ( $c_p$ ). Relations between  $w'$ ,  $u'$ ,  $p'$ , and  $\theta'$  as expressed by (3.5.16) and (3.5.17) are also sketched. Symbols H and L denote the perturbation high and low pressures, respectively, while W and C denote the warmest and coldest regions, respectively, for the wave at  $t_1$ . Symbol  $\alpha$  defined in (3.5.13) represents the angle of the wave number vector  $\mathbf{k}$  from the horizontal axis or the wave front (line of constant phase) from the vertical axis. (Adapted after Hooke 1986.)

waves with constant  $\omega < N$  propagate at a fixed angle to the horizontal axis, which is independent of the wavelength.

From (3.5.12), we may obtain the horizontal and vertical phase velocities,

$$c_{px} = \frac{\omega}{k} = \frac{\pm N}{\sqrt{k^2 + m^2}}; \quad c_{pz} = \frac{\omega}{m} = \frac{\mp kN}{m\sqrt{k^2 + m^2}} \quad (3.5.14)$$

These expressions indicate that pure gravity waves are dispersive in both the  $x$  and  $z$  directions because both  $c_{px}$  and  $c_{pz}$  depend on wave number. The group velocities can be derived from (3.5.12),

$$c_{gx} = \frac{\partial \omega}{\partial k} = \frac{\pm m^2 N}{(k^2 + m^2)^{3/2}}; \quad c_{gz} = \frac{\partial \omega}{\partial m} = \frac{\mp kmN}{(k^2 + m^2)^{3/2}}. \quad (3.5.15)$$

Note that  $c_{px}$  and  $c_{gx}$  are directed in the same direction, while  $c_{pz}$  and  $c_{gz}$  are directed in opposite directions. This is also shown in Fig. 3.9. Due to these peculiar properties of internal gravity waves, the implementations for lateral and upper boundary conditions associated with mesoscale numerical models that resolve these waves must be carefully configured. Briefly speaking, a horizontal advection equation,  $\partial \varphi / \partial t + c_{px} \partial \varphi / \partial x = 0$ , where  $\varphi$  represents any prognostic dependent variable, can be applied at the lateral boundaries and can be implemented to help advect the wave energy out of the lateral

boundary of the computational domain. On the other hand, a vertical advection equation,  $\partial\varphi/\partial t + c_{pz}\partial\varphi/\partial z = 0$  (with  $c_{pz} > 0$ ), cannot advect the wave energy out of the upper boundary since the wave energy will propagate downward back into the computational domain as is  $c_{gz}$  negative. The numerical radiation boundary conditions will be discussed in more detail in Section 13.2, while the details of the Sommerfeld (1949) radiation boundary condition will be discussed in Section 4.4.

Due to the fact that only the real part of the solution is physical, (3.5.6) and  $\hat{w}(z) = w_o \exp(imz)$  can be combined in the form,

$$w' = \text{Re}\left(w_o e^{i(kx+mz-\omega t)}\right) = w_r \cos(kx + mz - \omega t) - w_i \sin(kx + mz - \omega t), \quad (3.5.16)$$

where  $w_r$  and  $w_i$  are the real and imaginary parts of  $w_o$ , respectively. Substituting  $w'$  into (3.5.1)–(3.5.4) with  $U = 0$  leads to the *polarization relations*

$$u' = -(m/k)[w_r \cos(kx + mz - \omega t) - w_i \sin(kx + mz - \omega t)], \quad (3.5.17a)$$

$$p' = -(\rho_o \omega m/k^2)[w_r \cos(kx + mz - \omega t) - w_i \sin(kx + mz - \omega t)], \quad (3.5.17b)$$

$$\theta' = (\theta_o N^2/g\omega)[w_r \sin(kx + mz - \omega t) + w_i \cos(kx + mz - \omega t)]. \quad (3.5.17c)$$

The above relationships are also shown in Fig. 3.9 for the case where  $k > 0$ ,  $m < 0$ , and  $\omega > 0$ . The wave frequency is assumed to be positive, in order to avoid redundant solutions. For  $k > 0$ ,  $m < 0$ , and  $\omega > 0$ , (3.5.17a) indicates that  $u'$  is in phase with  $w'$ , which is shown in Fig. 3.9 by fluid oscillating toward the right in regions of upward motion. Equation (3.5.17b) indicates that  $p'$  is also in phase with  $w'$ . Thus, high (low) pressure is produced in regions of upward (downward) motion. Equation (3.5.17c) indicates that  $\theta'$  is out of phase with  $w'$  by  $\pi/2$  ( $90^\circ$ ). Fluid particles lose (gain) buoyancy in regions of upward (downward) motion, according to (3.5.4) with  $U = 0$ . Therefore, the least buoyant (coldest) fluid parcels (denoted by C in  $t_1$  of Fig. 3.9) will move toward regions of maximum upward motion. That is, internal gravity waves will move in the direction of phase propagation (toward the lower right corner of the figure), as denoted by  $c_p$  in the figure.

Returning to the vertical structure solutions, (3.5.8) and (3.5.9), there are two extreme cases that merit further discussion. When  $N^2 \gg \Omega^2$ , the buoyancy oscillation period ( $2\pi/N$ ) is much shorter than the oscillation period of the disturbance ( $2\pi/\omega$ ) or the advection time ( $L/U$ ). Therefore, the wave energy will propagate purely in the vertical direction. In this situation, constant phase lines and group velocities are oriented vertically, while the total wave number vector is oriented horizontally. In this special flow regime, often referred to as the *hydrostatic gravity wave regime*, the vertical momentum equation (3.5.2) reduces to its hydrostatic form,

$$\frac{1}{\rho_o} \frac{\partial p'}{\partial z} = g \frac{\theta'}{\theta_o}. \quad (3.5.18)$$

This implies that the vertical pressure gradient force is in balance with the buoyancy force in the  $z$  direction. In other words, vertical acceleration  $Dw'/Dt$  plays an insignificant role in wave propagation. It can be shown from (3.5.8) that the waves repeat themselves in the vertical direction without losing their amplitude and have a wavelength of  $2\pi\Omega/kN$  for a steady-state flow. For hydrostatic gravity waves, the wave equation (3.5.5) for the vertical velocity  $w'$  reduces to

$$\left(\frac{\partial}{\partial t} + U\frac{\partial}{\partial x}\right)^2 \frac{\partial^2 w'}{\partial z^2} + N^2 \frac{\partial^2 w'}{\partial x^2} = 0. \quad (3.5.19)$$

In the other limit,  $N^2 \ll \Omega^2$ , the buoyancy oscillation period is much greater than that of the disturbance ( $2\pi/\omega$ ) or advection time of the air parcel ( $L/U$ ). Therefore, the buoyancy force plays an insignificant role in this flow regime. In this situation, the wave energy is not able to propagate vertically, and the wave disturbance will remain locally in the vicinity of the forcing. The vertical momentum equation, (3.5.2), reduces to

$$\frac{\partial w'}{\partial t} + U\frac{\partial w'}{\partial x} = -\frac{1}{\rho_0} \frac{\partial p'}{\partial z}. \quad (3.5.20)$$

Thus, only the vertical pressure gradient force contributes to the vertical acceleration. It can also be shown from (3.5.9) that the amplitude of the disturbance decreases exponentially with height. As discussed earlier, this special case is called the *evanescent flow regime*. The wave equation for  $w'$  reduces to

$$\left(\frac{\partial}{\partial t} + U\frac{\partial}{\partial x}\right)^2 \left(\frac{\partial^2 w'}{\partial x^2} + \frac{\partial^2 w'}{\partial z^2}\right) = 0. \quad (3.5.21)$$

If the flow starts with no relative vorticity in the  $y$ -direction (i.e. if  $\partial u'/\partial z - \partial w'/\partial x = 0$  at  $t = 0$ ), then the above equation reduces to a two-dimensional form of the Laplace's equation

$$\frac{\partial^2 w'}{\partial x^2} + \frac{\partial^2 w'}{\partial z^2} = 0. \quad (3.5.22)$$

Because this type of flow is everywhere vorticity-free, it is often referred to as *potential (irrotational) flow*.

### 3.6 Inertia-gravity waves

When the Rossby number ( $R_o = U/fL$ ) becomes smaller, rotational effects need to be considered. In this situation, buoyancy and Coriolis forces can act together as restoring forces and inertia-gravity waves can be generated. The governing equations are similar to (3.5.1)–(3.5.4), but with three-dimensional and rotational effects included,